Numerical modelling of dynamic response of underground openings under blasting based on field tests

C.P. Yi, Luleå University of Technology, Sweden

P. Zhang, Luleå University of Technology, Sweden

E. Nordlund, Luleå University of Technology, Sweden

S. Shirzadegan, Luleå University of Technology, Sweden

U. Nyberg, Luleå University of Technology, Sweden

Abstract

In order to assess the capacity of ground support systems when subjected to dynamic loading, simulated rockburst tests by using blasting have been conducted at LKAB Kiirunavaara underground mine. In this paper, a numerical simulation for one of the field tests is conducted using LS-DYNA code to numerically investigate the effect of the different aspects of the charge design including the initiation point and the geometry on the test results. In the simulation, an explosive material model is used to model the detonation of explosive used in field tests and the Riedel-Hiermaier -Thoma (RHT) material model is used to model the dynamic response of the rock mass. The decoupling effect between the explosive and the wall of borehole is also taken into account in the model. The numerical results show a similar particle vibration pattern and a crack pattern to those of the field measurment. The effects of the position of the initiation point and the charge structure on the dynamic response of rock mass are also discussed. The results can be a reference for blast design for future field tests.

1 Introduction

Rockburst risk is an increasing problem in the underground mining worldwide, as the general trend is for mines to operate in deeper environments. In most mines affected by seismicity, the first line of defence to mitigate the potential consequences of rockburst is to install dynamic resistant ground support systems (Potvin, 2010). In order to assess the performance of ground support components and systems when submitted to seismic activity and strong ground motion, laboratory tests on core, drop test facilities, simulated rockburst experiments and passive monitoring and back analysis for case studies have been employed for many years in different countries (Hadjigeorgiou and Potvin, 2007).

Drop test and simulated rockbursts by blasting are two popular ways to test and understand the behavior of ground support elements when subjected to dynamic loads. Simulated rockbursts using blasting are generally performed underground in operating mines and they are destructive tests. Although the logistics of setting up and carrying out the tests are complicated and the cost is high compared to drop tests, the advantage is that the ground support is installed and tested in situ and tested as a system rather than individual support elements. Issues such as the interaction with the rock mass and installation procedures are also well simulated and weaknesses in the overall system are highlighted. A lot of simulated rockburst experiments using blasting have been carried out (Ortlepp, 1992; Tannant et al., 1995; Hagan et al., 2001; Espley et al., 2002; Archibald et al., 2003; Andrieux et al., 2005; Heal and Potvin, 2007).

Numerical modelling was used in both the forward planning and the back-analysis of simulated rockburst experiments. Modelling was used to give insight into the design of the experiment, the blast and the positioning of monitoring equipment. Hildyard and Milev (2001) developed a numerical model for seismic wave propagation from the blast to model an artificial rockburst experiment. In their model, the dynamic load consists of applying dilatational pressure ($\sigma_1=\sigma_2=\sigma_3$) along a line of grid-points within the solid material

of a finite difference mesh. The charge-length and diameter are directly related to the length of the line and the grid-point spacing in the finite difference implementation. Larger diameters are modelled by pressurizing parallel lines or a volume of grid-points. The pressure function describes how the pressure at a point in the source varies with time. The phase of this pressure function varies along the charge line. Minkley (2004) modeled a simulated rockburst using UDEC code. A pressure impulse was used to represent a blasting load in his model. Zhang et al (2013) conducted a back-analyzing for the test results using coupled numerical modeling technique. The blasting is simulated by using finite element method (LS-DYNA) and the dynamic interaction between blasting generated waves and rock mass is simulated by using discrete element modeling (UDEC) with the dynamic input from LS-DYNA (Hallquist 2013). In these studies, the blasting source was represented by an equivalent load form which cannot accurately represent the detonation process of explosive in blastholes and the expansion of detonation products. Especially, only P-waves radiate from the loading boundaries for a two-dimensional model because the velocity of detonation (VoD) in a 2-D model is implied as infinite. However, the investigation of Heelan (1953) indicates that a relatively large amount of the radiated energy from a borehole goes into S-waves, while the rest of it goes into P-waves. It is important to correctly describe the blast load for numerical modelling.

During 2010-2013, a series of underground experiments were conducted at the Kiirunavaara underground iron ore mine which is owned by Luossavaara-Kiirunavaara AB (LKAB) and located in Kiruna, Sweden (Shirzadegan, 2014). The principal objective of the simulated rockburst experiments has been to assess the in-situ performance of different ground support systems under dynamic loading. It is surprising that very high peak particle vibration velocity (PPV) (7.5 m/s) near the sidewall surface were obtained, but with little damage to the support system. With the gradual increase of explosive charge and slight adjustment of burden, the whole tested panel was then fully destroyed. Why it causes such totally different results is not clear yet and most importantly how to design blast in order to effectively investigate the support systems become extremely tough.

In this paper, Test 2 in Shirzadegan (2014) is numerically investigated using the LS-DYNA code. The blast load is directly modeled with an explosive model in LS-DYNA. The crack pattern and the particle vibration velocity are compared to the experimental results.

2 Numerical model

2.1 Descriptions of the model

The southern wall of the cross-cut 93 located in block 9 mining level 741 m was selected to conduct Test 2. The size of the cross-cut was 7.0 m (W_{cc}) in width and 5.2 m (H_{cc}) in height and the width of the adjacent pillar was approximately 18m, see Figure 1. Rock types in the tested area comprised 'syenite porphyries' (mainly trachytes to trachyandesites) of variable character. The blasthole was drilled from the adjacent footwall drift in a direction parallel to the crosscut and was around 15 m long. The diameter of the blasthole was 152mm and the average distance (burden) of the blasthole to the test wall was 3.9m. The height of the blasthole to the floor (H_{bh}) was 1.6 m. Two different charge concentrations, each one around 5 m in length, were used inside the blasthole for generating different dynamic loads on the panel in one blast. The charge diameter of the high and low charge segments were 98 mm and 76 mm respectively, indicating to a decoupled charge structure with different decoupling ratios. The length of each charge segment was 5 m. The blasthole was toe primed and was left unstemmed to vent the detonation gas and further reduce the effect of detonation gas. The used explosive was NSP711. The reasons for selecting this explosive were the lower amount of gas production compared to other commercial explosives, high VOD and blasthole pressure resulting in getting more energy through shock wave than the gas expansion (Zhang et al. 2013).

According to the in-situ test, a numerical model was generated with Truegrid software (Rainsberger 2006), see Figure 2. The reinforcement at the tunnel wall is not considered in this model. The difference between the numerical model and the field experiment is that the blasthole is located at the left side of the drift in

the numerical model. This model consists of approximate 15 million hexahedral elements and the element size is roughly 5cm. A Massively Parallel Processing (MPP) version LS-DYNA solver was used to run this case. The numerical model was divided into several blocks and each part was represented in different colors, which is for the convenience to select the nodes which correspond to the locations of the accelerometers installed. All blocks which represent the rocks have exactly the same parameters.

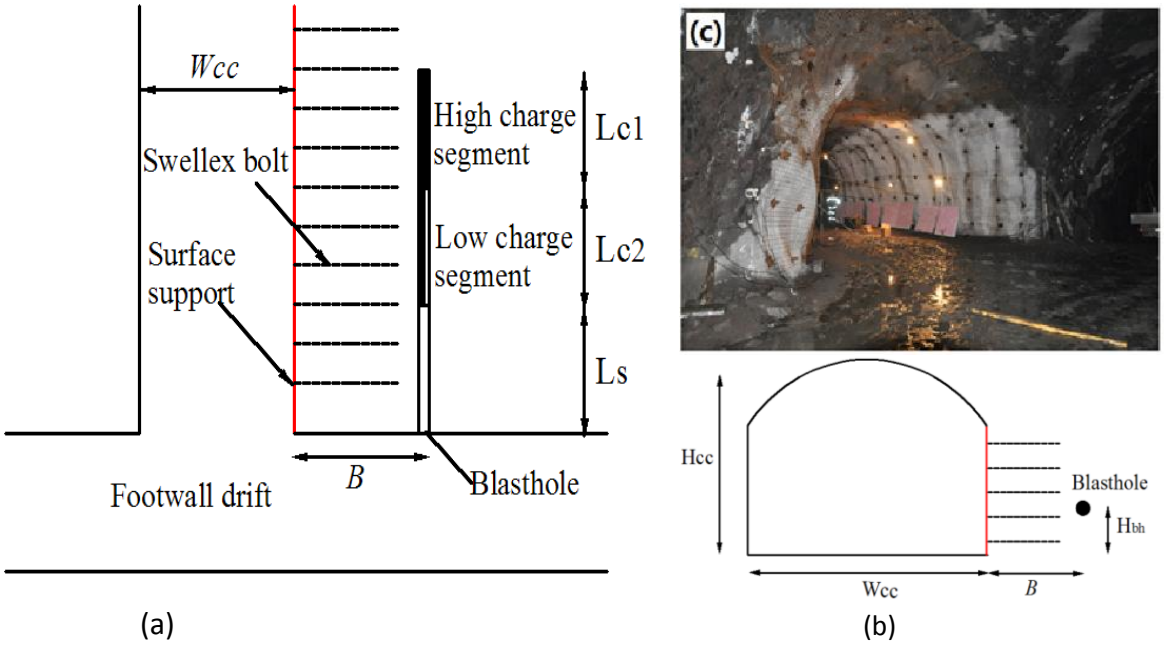

Figure 1 Schematic diagram of test layout and blast design. (a) Top view, (b) front view and (c) photo of instrumented side wall in Test 2

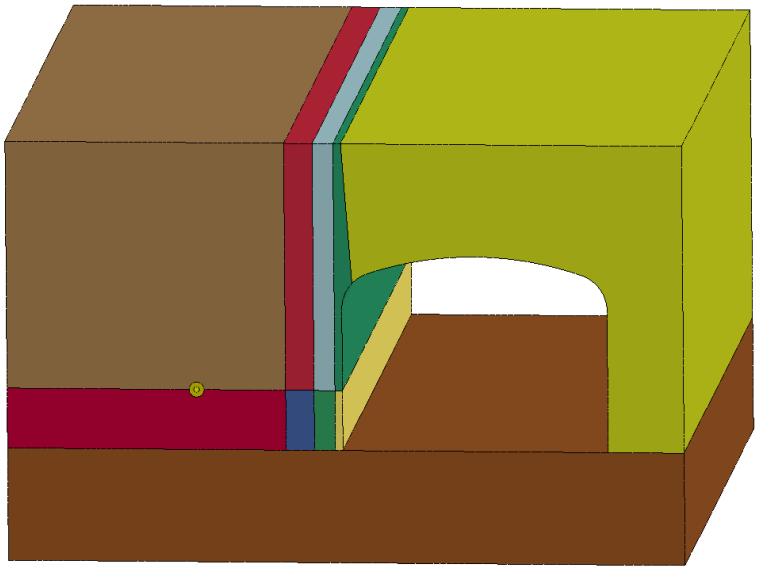

Figure 2 LS-DYNA model

2.2 Material properties for modelling

The NSP 711 explosive used in the field test is modeled with an explosive material model in LS-DYNA and with the Jones-Wilkins-Lee (JWL) equation of state (EoS) (Lee et al., 1968) as Eq. (1).

$$p = A\left(1-\frac{w}{R_1V}\right)e^{-R_1V} + B\left(1-\frac{w}{R_2V}\right)e^{-R_2V} + \frac{wE_e}{V} \quad (1)$$

where *p* is the pressure; *A, B, R_1, R_2* and *w* are constants and *V* and E_e are the specific volume and the internal energy respectively. In eq.(1), *A, B,* and E_e have units of pressure while *R1, R2,* and *w* are unitless. The parameters of NSP 711 explosive were calibrated by Helte et al. (2006) and listed in Table 1. In Table 1, ρ is the density of the explosive used, *D* is the velocity of detonation of the explosive, P_{CJ} is the Chapman-Jouguet pressure of the explosive.

Table 1 Parameters of NSP 711 explosive

ρ (kg/m³)	*D*(m/s)	P_{CJ}(GPa)	*A* (GPa)	*B(GPa)*	R_1	R_2	*w*	E_e(KJ/cc)
1500	7680	21.15	759.9	12.56	5.1	1.5	0.29	7.05

As mentioned before, the charge structure in the blasthole is decoupling. The gap between the explosive and the wall of the blasthole was filled with air. *MAT_NULL is adopted for air and is combined with a linear polynomial EoS shown in equation (2).

$$P=\left[C_0+C_1\mu+C_2\mu^2+C_3\mu^3\right]+\left[C_4+C_5\mu+C_6\mu^2\right]E_0 \tag{2}$$

where C_0, C_1, C_2, C_3, C_4, C_5, and C_6 are constants and $\mu=\frac{\rho}{\rho_0}-1$ with $\frac{\rho}{\rho_0}$ the ratio of current density to initial density, E_0 is initial internal energy per unit reference volume. For gases which the gamma law EoS applies such as air, therefore eq (2) reduces to $P=(\gamma-1)\frac{\rho}{\rho_0}E_0$. For *MAT_NULL, a pressure P_C is used to limit the amount of pressure that can be generated by tensile loading. This pressure was set to zero since air does not allow tension. Similarly, since the inertial forces were dominant, the flow was assumed to be inviscid and thus the dynamic viscosity coefficient μ_c could be omitted. All the used parameters for air are given in Table 2. V_0 is the initial relative volume of air in Table 2.

Table 2 Parameters of air (Olovsson et al. 2003)

ρ (kg/m³)	P_C	μ_c	C_0-C_3, C_6	C_4	C_5	γ	E_0 (MPa)	V_0
1.29	0	0	0	0.4	0.4	1.4	0.25	1.0

The rock mass is modeled with the RHT material model in LS-DYNA, which is an advanced plasticity model for brittle materials such as concrete and rock. It was proposed by Riedel et al. (Riedel et al., 1999) for dynamic loading of concrete and implemented in the LS-DYNA code by Borrvall and Riedel (2011). In the RHT model, the description of the stress state is based on the three invariants of the stress tensor for the definition of the elastic limit surface, failure surface and residual strength surface for the crushed material. These three surfaces all are pressure dependent. In this model, the damage is defined using $\mathrm{D}=\sum\frac{\Delta\varepsilon^{\mathrm{p}}}{\varepsilon^{\mathrm{f}}}$, where $\Delta\varepsilon^{\mathrm{p}}$ is the accumulated plastic strain $\mathrm{and}\ \varepsilon^{f}$ is the failure strain. Some of used values for the modeling of the rock are shown in Table3. Here, ρ is the density of the rock mass, E is the elastic modulus, σ_c is the uniaxial compressive strength, σ_t is the uniaxial tensile strength and v is the Poisson's ratio.

Table 3 Parameters of rock mass.

ρ (kg/m³)	E (GPa)	σ_c (MPa)	σ_t (MPa)	v
2800	70	180	10	0.27

3 Numerical results

3.1 Vibration velocity analysis

In Test 2, Accelerometer 9 was located at 0.2 m behind the middle of the panel surface (the high charge segment) and their heights were close to the height of the axis of blasthole. The integrated velocity–time

curve for Accelerometer 9 is plotted in Figure 9 (a) together with the numerical result of a node which corresponds to the position of Accelerometer 9. Also the velocity integrated from the record of accelerometer 18 located 0.75 m behind the surface is compared with numerical modelling and plotted in Figure 9 (b).

In both cases, the PPV from the numerical modelling is lower than that from the field test. One possible reason is that the zone near the surface of the side wall is a fractured zone due to the excavation of the drift by blasting. The investigation of Zhang et al (2015) indicates that the presence of a fractured zone near the surface of the wall can amplify the PPV. It can also be observed that the duration of the velocity-time curve from the numerical modelling is shorter than that from the field test. At the beginning of the vibration velocity curves, the field result and the numerical result have the similar rise rate and the similar waveform.

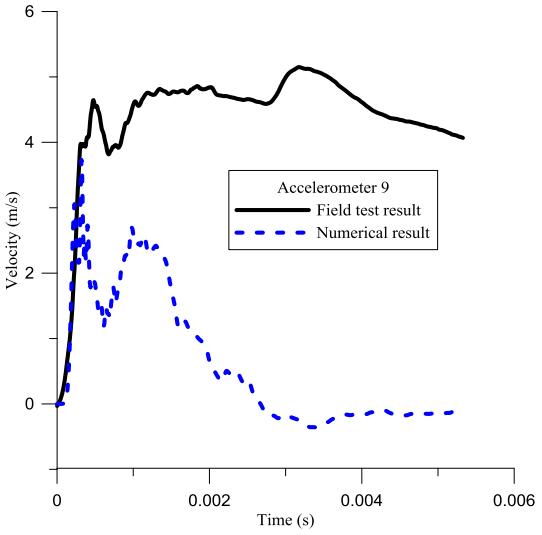

(a) Velocity of Accelerometer 9

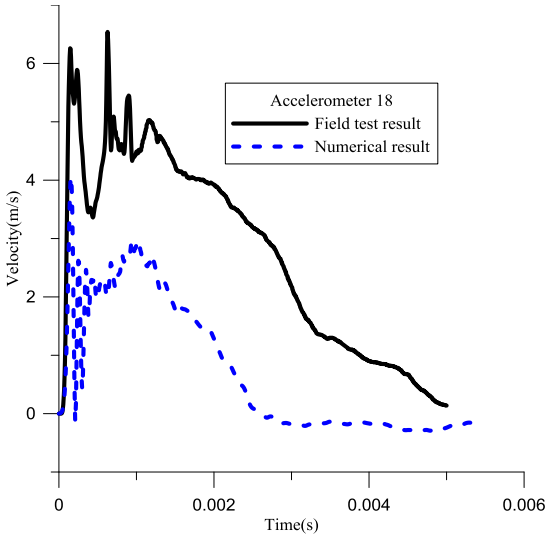

(b) Velocity of Accelerometer 18

Figure 3 Vibration velocities at different positions from field test and numerical modelling

3.2 Displacement distribution

The displacement distribution at 6 ms on the surface of the side wall is shown in Figure 4 (a) and the displacement distribution at the section behind 0.2m of the surface of the side wall is shown in Figure4 (b). It can be seen that the peak displacement of the side wall is 2.4 cm and it is 1.75cm on the section behind 0.2m of the side wall. Displacements from the numerical modelling are smaller than those from the field measurements (Shirzadegan, 2014). One possible reason is that the rock is simulated as continuous material. The numerical results show that the large displacement areas in Figures 4 (a) and 4 (b) are around the join point of the high charge segment and the low charge segment.

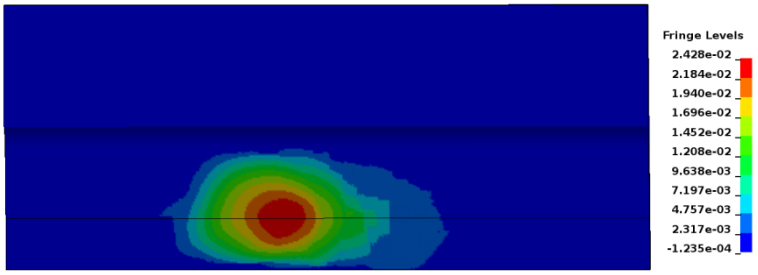

(a) Displacement distribution on the surface of the side wall at 6ms

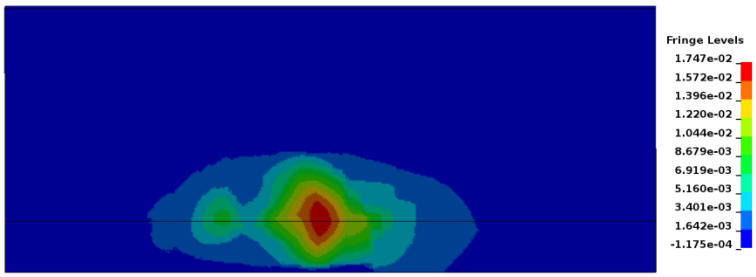

(b) Displacement distribution on the plane at 0.2m behind the side wall at 6ms

Figure 4 Displacement distributions in different sections

3.3 Crack pattern

After the blasting, the damage distribution in the rock mass is shown in Figure 5 (a). It is hard for finite element method to directly model the initiation and propagation of cracks in rock mass. In this paper, the elements with damage level above 0.7 were blanked out to form cracks in the rock mass after blasting. The crack pattern is shown in Figure 5 (b). The damage on the panel in Test 2 is shown in Figure 5 (c).

It should be noted that the side wall is on the left side of the blast hole in the field test while it is on the right side of the blast hole in the numerical model. So the directions of crack from the field test and the numerical modelling are consistent.

Two cross-sections are chosen in Figure 6 to show the internal cracks. Figure 6 indicates that radial cracks are the dominate crack around the blast hole. The depth of the crack on the surface of the side wall is small. The failure of the side wall of drift is because of the reflection of stress waves.

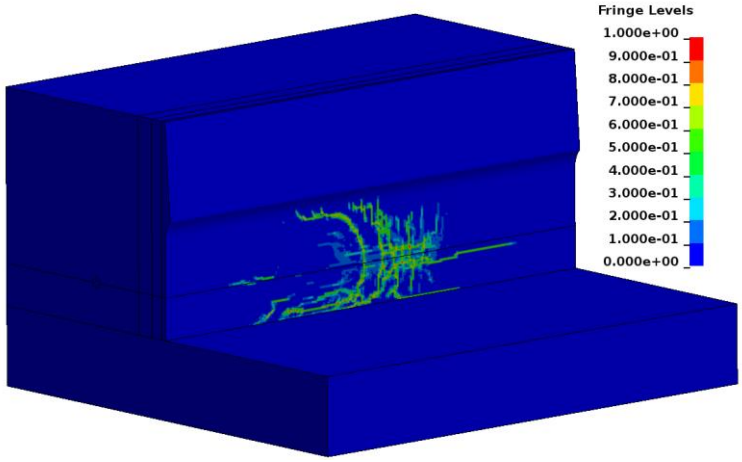

(a) Damage distribution in the rock mass

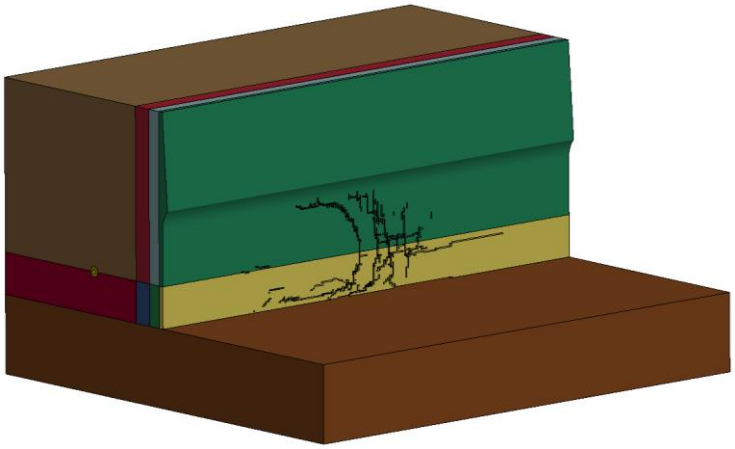

(b) Overall crack pattern

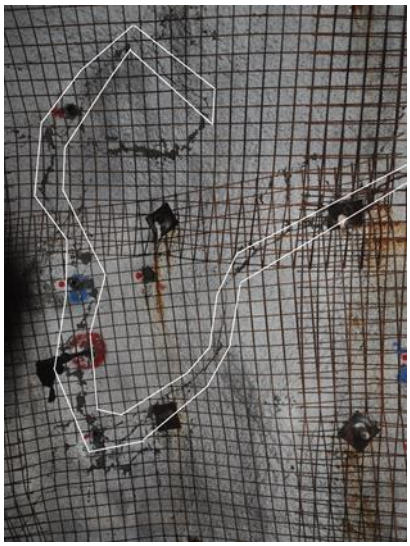

(c) Damage on the panel in Test 2

Figure 5 Damage on the panel from numerical modelling and field test

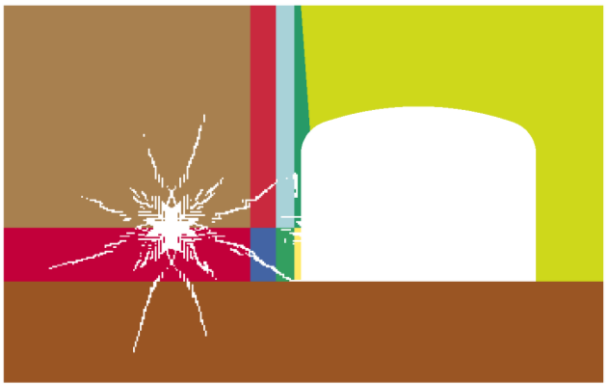

(a) Cross-section at the middle of the high charge segment

(b) Cross-section at the middle of the low charge segment

Figure 6 Internal crack patterns at different cross-sections

4 Discussion

Although using blasting to simulate the effects of rockbursts on ground support systems has been used by many researchers, until now, there is no standard on how to conduct simulated rockburst experiments and different blast designs have been utilized in existing simulated rockburst experiments. The dynamic response of rock mass under blasting depends on several factors such as burden, the amount of charge, the position of initiation point, the charge structure and so on. It is good to know how these factors affect the results for a blast design.

4.1 Effect of the position of initiation point

The low charge segment was close to the open end of the blast hole while the high charge segment was loaded near the toe of the blast hole in Test 2. The detonator is located at the toe of the blast hole. The field measurements indicated that the most of the large PPVs are located in the area which corresponds to the low charge segment (Shirzadegan, 2014). Numerical results also show the similar phenomenon. A lot of factors can affect the dynamic response of rock mass under blasting. The position of the initiation point could be one of the reasons for this phenomenon. To investigate the effect of the position of the initiation point, a case that the initiation point is located at the end of the low charge segment was run.

Two nodes that were located at the surface of the side wall and correspond to the middle of different charge segments are selected to compare their vibration response. Node 11092102 corresponds to the low charge segment while Node 11092203 corresponds to the high charge segment. When the initiation point is located at the toe of the blast hole, the stress wave due to blasting reaches Node 11092203 first and then Node 11092102, see Figure 7 (a). The PPV of Node 11092203 is smaller than that of Node 11092102. When the initiation point is located at the end of the low charge segment, the stress wave reaches Node 11092102 first and then Node 11092203, see Figure 7 (b). The PPV of Node 11092102 is smaller than that of Node 11092203.

According to the numerical modelling, when two different charge concentrations are used inside the blast hole to generate different dynamic loads on the panel in one blast, it could be hard to tell the difference between two dynamic loads from different charge concentrations.

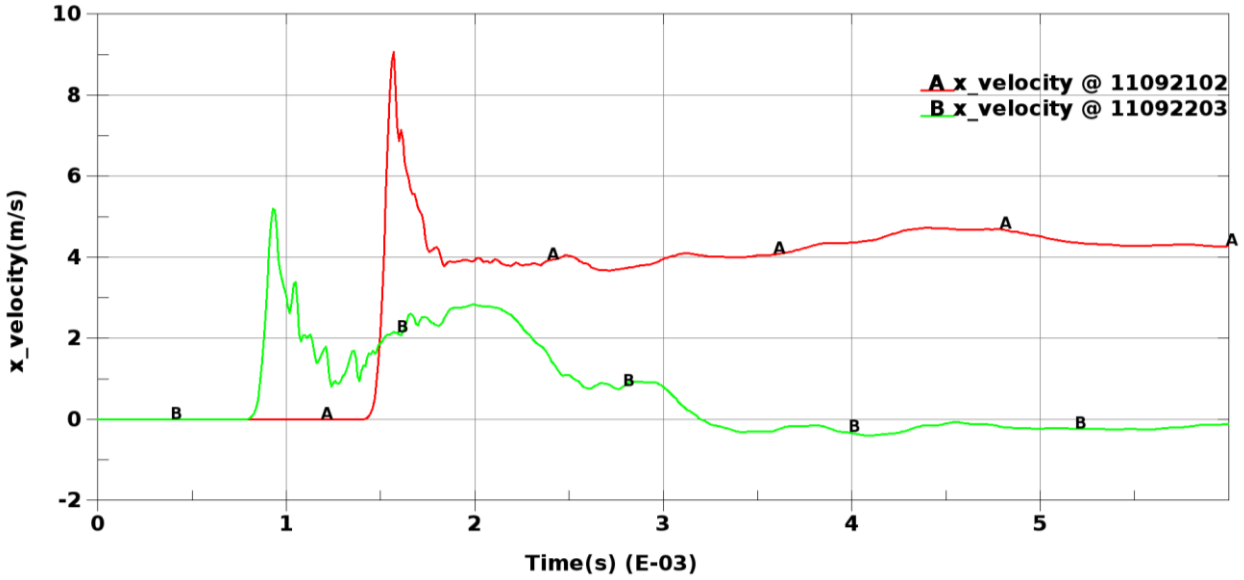

(a) The initiation point is located at the toe of the blast hole

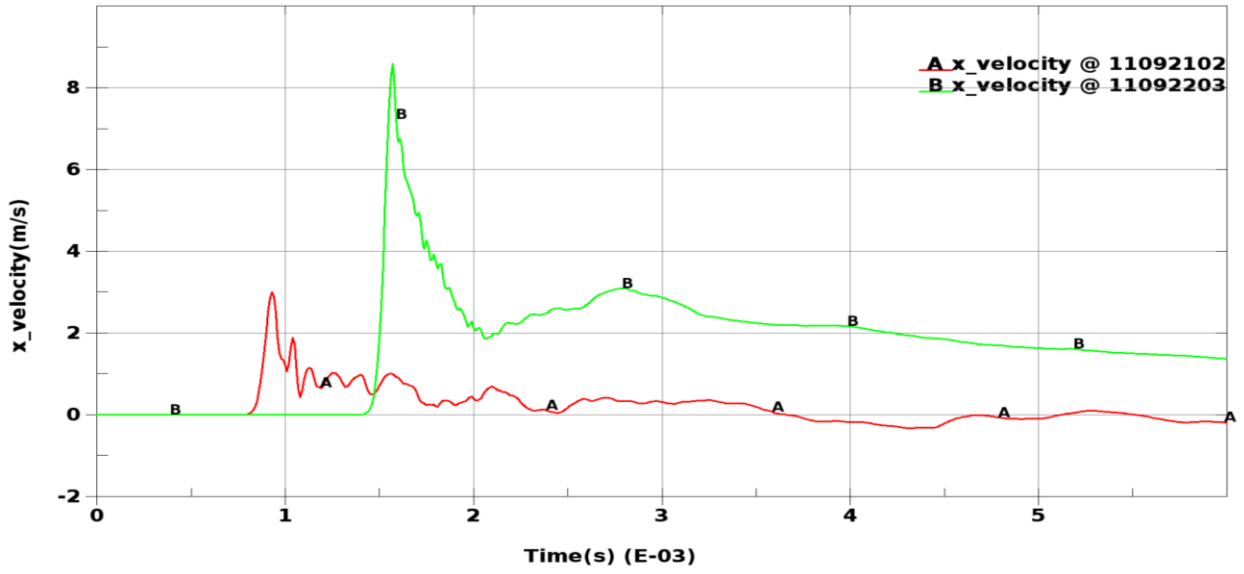

(b) The initiation point is located at the end of the low charge segment

Figure 7 Comparison of vibration velocities for different initiation points

4.2 Effect of charge structure

In Test 2, the high charge segment was located at the bottom of the blast hole. To investigate the effect of charge structure, two cases were investigated numerically. One case is that two charge segments in Section 3 exchange their locations, and the other case is that two charge segments have the same diameter of 98 mm. The initiation point for two cases was located at the toe of the blast hole. The crack patterns of two cases are shown in Figure 8.

Comparison between Figure 8 and Figure5 (b) shows that different charge structures induce different crack patterns.

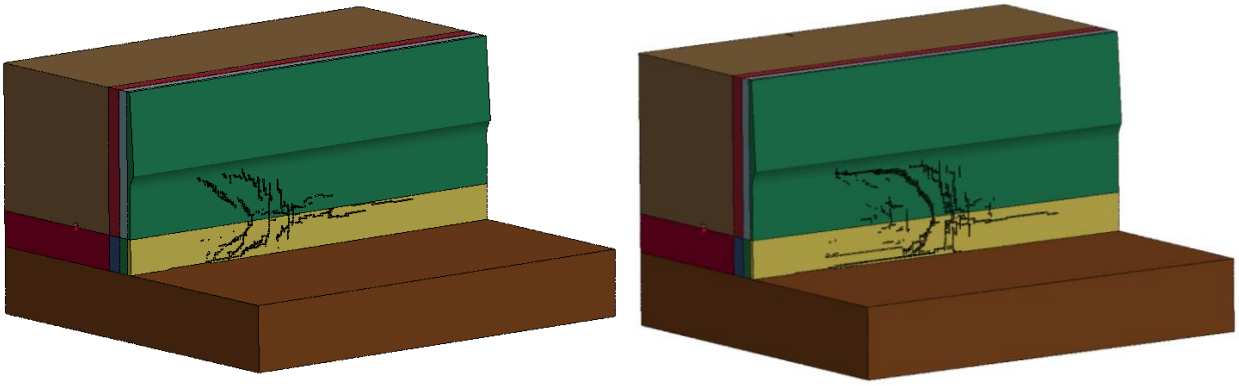

(a) Crack pattern after exchanging locations (b) Crack pattern of same charge diameter

Figure 8 Crack patterns for different charge structures

The same nodes as those in Section 3 were selected to plot their velocity-time curves. Results are shown in Figure 9. The PPV of node 11092203 in Figure 9 (a) is less than that in Figure 9 (b). It is because that Node 11092203 in Figure 9 (a) corresponds to the low charge segment, which means the PPV is also related to the charge concentration of explosive. Figure9 (b) also indicates that the vibration response of rock mass is related to the direction of detonation propagation.

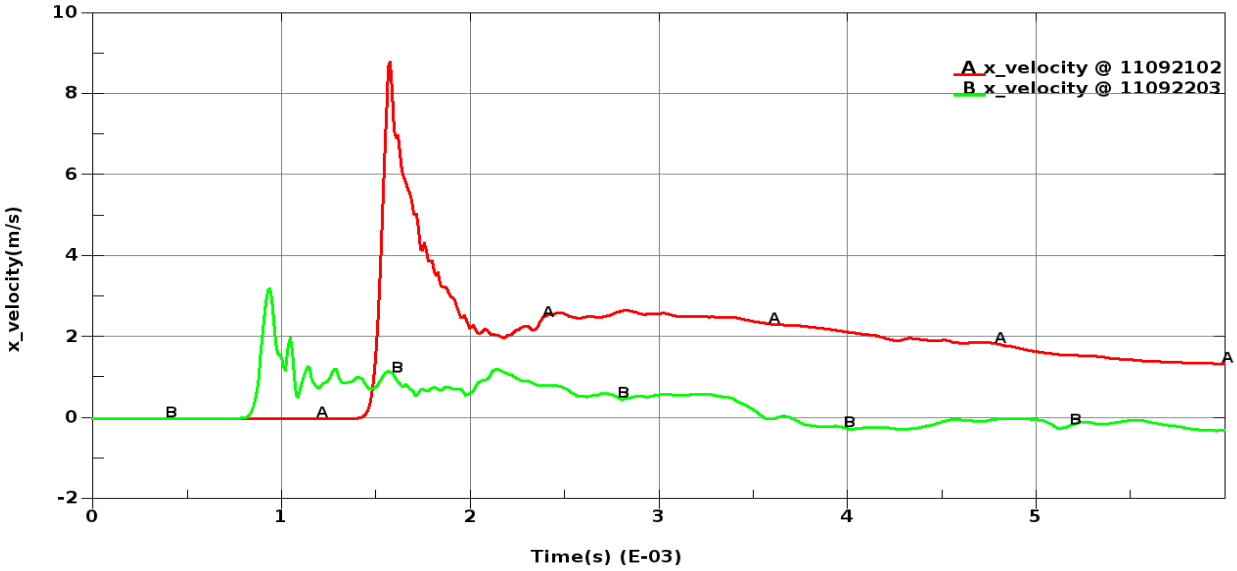

(a) Two charge segments exchange locations

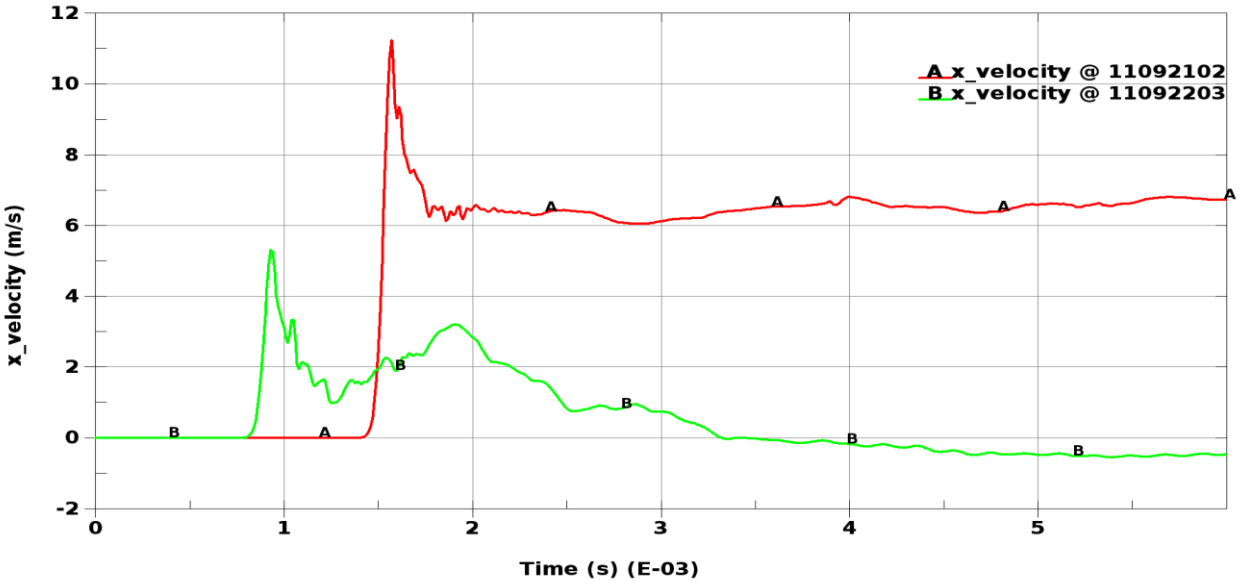

(b) Two charge segments have the same diameter

Figure 9 Velocity-time curves due to different charge structures

4.3 Limitations of the numerical modelling

Although LS-DYNA can model the detonation of explosive and the dynamic response of rock mass due to blasting, and the 3-D model can also avoid omitting the effect of shear waves, the spalling of the side wall due to blasting cannot be modelled directly because of the limitations of continuum-based methods.

The ground support was not simulated in this paper. The model will be complicated if the shotcrete and the rebars are added into the model. Zhang et al. (2013) stated that PPVs are not greatly affected when support system is applied, because the shock wave hits the panel rapidly, the support will first move together with the rock mass as a whole without restraining the rock mass markedly before fractures are generated.

The presence of discontinuities in rock mass greatly affects the propagation of stress wave due to blasting. The existing natural discontinuities in rock mass were not taken into account in the numerical model, which could be one of the reasons for the discrepancies regarding velocity and displacement between numerical modelling and field measurements.

5 Conclusion

In order to better understand the results of the simulated rockburst test conducted at Kiirunavaara underground mine, LS-DYNA code has been used to numerically investigate one of the tests. Based on the simulations it can be concluded that:

1) Numerical results indicated to the similar waveform at the beginning of the vibration velocity curve and the similar PPVs distribution to the field measurement. The crack pattern from the field test and the numerical modelling were similar. It could be possible to improve the blast design for the simulated rockburst test by using numerical modelling.

2) The dynamic response of rock mass under blasting strongly depends on the position of the initiation point, the charge structure and the charge concentration. Numerical results show that the PPVs on the tested panel increase along the direction of detonation propagation. It is hard to investigate the effect of different dynamic loads by using different charge concentrations in one blasthole.

References

Andrieux, P., Turichshev, A., O'Connor, P & Brummer, R.K 2005, 'Dynamic testing with explosive charges of rockburst-resistant ground support systems at the Fraser Nickel Mine', Itasca Consulting Canada Inc Report to Falconbridge Limited MineTechnical Services; Final Version, September 2005, Sudbury, Canada, 102 p.

Archibald, J.F., Baidoe, J.P & Katsabanis, P.T 2003, 'Rockburst damage mitigation benefits deriving from use of spray-on rocklinings, Surface Support in Mining', in Y. Potvin, T.R. Stacey and J. Hadjigeorgiou (eds), Australian Centre for Geomechanics,Perth, pp. 169–178.

Borrvall, T. & Riedel, W. 2011. 'The RHT concrete model in LS-DYNA'. 8th European LS-DYNA users conference. Strasbourg.

Espley, S.J., Heilig, J & Moreau, L.H 2002, 'Assessment of the dynamic capacity of liners for possible application in highly stressed mining environments at Inco limited, Surface Support in Mining', in Y. Potvin, T.R. Stacey & J. Hadjigeorgiou (eds), Australian Centre for Geomechanics, Perth, pp. 187–192.

Hadjigeorgiou, J & Potvin, Y 2007, 'Overview of dynamic testing of ground support', in Y. Potvin (ed), Proceedings Fourth International Seminar on Deep and High Stress Mining (Deep Mining 07), Perth, Australia, pp. 349–371.

Hagan, T.O., Milev, A.M., Spottiswoode, S.M., Hildyard, M.W., Grodner, M.A., Rorke, J., Finnie, G.J., Reddy, N., Haile, A.T., Le Bron,K.B. & Grave, D.M 2001, 'Simulated rockburst experiment – an overview', The Journal of The South African Institute of Mining and Metallurgy, August 2001, pp. 217–222.

Hallquist, J 2013. ' LS-DYNA keyword user's manual'. Livermore software technology corporation, LSTC, Vol. 1 & 2.

Heal, D & Potvin, Y 2007, 'In-situ dynamic testing of ground support using simulated rockbursts', in Y. Potvin (ed), Proceedings Fourth International Seminar on Deep and High Stress Mining (Deep Mining 07), Perth, Australia.

Heelan, P.A 1953. 'Radiation from a cylindrical source of finite length'. Geophysics, vol. 18,no.3: 685-696.

Helte, A., Lundgren, J., Örnhed, H & Norrefeldt, M 2006, 'Prestandabestämning av svensk sprängdeg m/46', rapport nr FOI-R--2051--SE, FOI, ISSN 1650-1942, Stockholm, September 2006.

Hildyard, M.W & Milev, A.M 2001, ' Simulated rockburst experiment: Development of a numerical model for seismic wave, propagation from the blast, and forward analysis', J S AFR I MIN METALL, vol.101, pp.235-245.

Hildyard, M.W & Milev, A.M 2001, 'Simulated rockburst experiment: Numerical back-analysis of seismic wave interaction with the tunnel', J S AFR I MIN METALL, vol.101, pp.223-234.

Lee, E.L., Horning, H.C. & Kury, J.W. 'A diabatic expansion of high explosives detonation products'. Lawrence Livermore National Laboratory, University of California, Livermore, TID4500-UCRL 50422. 1968.

Minkley,W 2004, 'Back analysis rock burst völkershausen 1989'. in Heinz Konietzky (eds), Numerical modelling of discrete material in geotechnical engineering, civil engineering and earth science, proceedings of the first international Udec/3Dec ,Bochum, Germany.

Olovsson, L., Souli, M. and Do,I 2003, 'Fluid-Structure Interaction Modeling with LS-DYNA', http://ftp.lstc.com/anonymous/outgoing/jday/aletutorial-278p.pdf.

Ortlepp, W 1992, 'Explosive-load testing of tunnel support, Rock Support in Mining and Underground Construction', in Kaiser, P.K.and McCreath, D.R. (eds), Balkema, Rotterdam, pp. 675–682.

Rainsberger, R 2006, ´TrueGrid User's Manual',V I&II, XYZ Scientific Applications, Inc.

Riedel, W., Thoma, K., Hiermaier, S. & Schmolinske, E. Penetration of reinforced concrete by BETA-B-500, numerical analysis using a new macroscopic concrete model for hydrocodes. In SKA (ed.), Proceedings of the 9th International Symposium on Interaction of the Effects of Munitions with Structures, Berlin. 1999.

Shirzadegan, S 2014, 'Development of a methodology for in-situ dynamic testing of ground support'. Licentiate thesis, Luleå University of Technology.

Tannant, D.D., Brummer, R.K. & Yi, X 1995, 'Rockbolt behaviour under dynamic loading: field tests and modelling', International Journal of Rock Mechanics and Mining Sciences & Geomechanics Abstracts, Vol. 32, pp. 537–550.

Zhang, P, Yi, C, Norlund, E, Shirzadegan, S & Nyberg, U 2013, 'Numerical back-analysis of simulated rockburst field tests by using coupled numerical technique'. in Y. Potvin and B. Brady (eds), Ground Support 2013 , Perth, Australia.

Zhang, P., Swan, G. &Nordlund, E 2015, '1D numerical simulation of velocity amplification of P-waves travelling through fractured rock near a free surface',The Journal of The Southern African Institute of Mining and Metallurgy.Vol.115, no. 11, pp. 1121-1126.